Biomaterials 33 (2012) 5848–5853

Contents lists available at SciVerse ScienceDirect

Biomaterials

journal homepage: www.elsevier.com/locate/biomaterials

The inhibition of tumor growth and metastasis by self-assembled nanofibers of taxol

Huaimin Wang [1], Jun Wei [1], Chengbiao Yang, Huiyuan Zhao, Dongxia Li, Zhinan Yin, Zhimou Yang*

State Key Laboratory of Medicinal Chemical Biology and College of Life Sciences, Nankai University. Tianjin 300071, PR China

ARTICLE INFO

Article history:
Received 5 March 2012
Accepted 22 April 2012
Available online 16 May 2012

Keywords:
Cancer therapy
Hydrogel
Self-assembly
Taxol

ABSTRACT

Molecular hydrogels have big potential for local delivery and sustained release of therapeutic agents. In this paper, we reported on a molecular hydrogel mainly formed by the widely used anti-cancer drug of taxol. The hydrogel was formed by an ester bond hydrolysis process from a taxol derivative (Taxol-SA-GSSG, **1**) and could be administrated into solid tumors to dramatically hinder their growths and prevent their metastasis. Besides the improved anti-cancer effect compared to the clinically used intravenous (i.v.) injection of Taxol®, the concentration of taxol in blood was low due to the local administration of taxol hydrogels, which greatly enhanced the dosage tolerance of mice to taxol and might reduce side effects of taxol during chemotherapy. Our observations suggested that the hydrogel mainly composed of taxol would have great potential for its practical applications.

© 2012 Elsevier Ltd. All rights reserved.

1. Introduction

We reported on a molecular hydrogel mainly formed by clinically used taxol without any chemical modifications. In order to overcome the shortcomings of anti-cancer drugs during chemotherapy (e.g. low water solubility and systemic toxicity), great efforts have been applied for the development of drug carriers that can improve the solubility of widely used anti-cancer drugs (e.g. taxol, camptothecin, and doxorubicin) and specifically deliver these drugs to cancer cells [1–6]. Besides the widely used polymeric hydrogels [7,8], nano-sized carriers such as liposomes, vesicles formed by DNA and block co-polymers and some inorganic materials [9–14], self-assembled molecular hydrogelators exhibited great potential for targeted or local delivery of hydrophobic anti-cancer drugs [15]. Stupp group have used a self-assembled peptide amphiphile to deliver Camptothecin to reduce the size of tumor [16], Pochan and co-workers also applied a peptide-based molecular hydrogel for local delivery of curcumin for chemotherapy [17], and John group have successfully constructed molecular hydrogelators by enzymes and developed enzyme-responsive hydrogels for the delivery of hydrophobic drug molecules [18,19]. Besides using molecular gelators as carriers for the delivery of anti-cancer drugs, Xu and our groups have recently reported several gelators based on taxol conjugates and these hydrogels of taxol derivatives might be developed into novel self-delivery systems for sustained release of taxol (gelators served as both carriers and delivered components) [20–22]

Though molecular hydrogels have shown promising potential for the delivery of anti-cancer drugs, the reported delivery systems are either with carriers (self-assembled molecules) or formed by drug derivatives, which need long time and cost more to evaluate the compatibility of carriers or compatibility and efficacy of drug derivatives. Actually, the only two FDA approval drug delivery systems of molecular hydrogels are those formed by therapeutic agents themselves (Lanreotide and Degarelix) without any chemical modifications [23,24]. Overall, molecular hydrogels formed by therapeutic agents themselves should have bigger potential for practical applications than other delivery systems with molecular hydrogels. In this paper, we reported on a molecular hydrogel mainly formed by taxol itself for local (intra-tumor (i.t.)) delivery of taxol with improved anti-tumor efficacy and lower systemic toxicity.

2. Materials and methods

2.1. Formation of hydrogel and its recovery property

20.0 mg of compound **1** and 2.2 equiv. of Na_2CO_3 (to **1**) were dissolved in 1.0 mL of PBS buffer (pH = 7.4), the gel would form being kept at 37 °C for 12 h. The gel could be imbibed to a syringe and then injected out from it. We observed the re-formation of a gel after 5 min.

2.2. Analysis of hydrolysis process during hydrogel formation

20.0 mg compound **1** and 2.2 equiv. of Na_2CO_3 were dissolved in 1.0 mL of PBS buffer (pH = 7.4). Tubes with 20 μL of the above solution were put at 37 °C. 200 μL of

* Corresponding author. Tel.: +86 22 23502875; fax: +86 22 23498775.
E-mail address: yangzm@nankai.edu.cn (Z. Yang).
[1] The authors contribute equally to this work.

0142-9612/$ – see front matter © 2012 Elsevier Ltd. All rights reserved.
doi:10.1016/j.biomaterials.2012.04.047

methanol was added at different time point, and then the clear solution was used to run LC-MS. The areas of peaks in LC-MS spectra were used to determine the percentage of hydrolysis of Taxol-SA-GSSG ($n = 4$, SD was determined).

2.3. In vitro release profile of taxol from the hydrogel

0.25 mL of gels (formed from 1.0 wt%, 1.5 wt%, and 2.0 wt% of **1** at 37 °C for 4 days) were treated with 0.25 mL of fresh PBS buffer solutions (pH = 7.4). A 0.20 mL of the upper buffer solution was taken out for LC-MS at each time point, and another 0.20 mL of fresh PBS buffer was added onto the top of the hydrogels. The areas of peaks in LC-MS spectra were used to determine the percentage of taxol released from their corresponding gels. The experiment was conducted in 4 parallel experiments.

2.4. In vivo drug toxicity

Mice were received s.c. injection of indicated dose of the hydrogels in the right flank. Mice weight was monitored every other day. And relative mice weight was calculated as: Relative Mice Weight = Weight/Original Weight × 100%.

2.5. In vivo Pharmacokinetics analysis

Three doses of our hydrogels (10, 20 and 40 mg/kg) in 50 μL PBS were s.c. injected in the right flank of age and sex-matched mice. Blood were collected at indicate time points. The treatment method was according with the reference. Briefly, 500 μL of Blood samples were collected in heparinized tube at the designated time intervals. The sample plasma was harvested by centrifugation at 1500 g for 10 min. Liquid–liquid extraction was performed to separate taxol from the plasma. Pharmacokinetic parameters were processed by software PKSolver.

2.6. In vivo evaluation of antitumor activity

EL-4 cells and 4T1-luciferase cells were maintained in our lab. For lymphoma model, C57BL/6J mice received s.c. injection of $2X10^5$ EL-4 cells; For breast tumor model, female Balb/c mice were inoculated with $2X10^5$ 4T1-luciferase cells in the mammary fat pad. Tumor growth was monitored every other day. Tumor volume was calculated by the formula: length × width × (Length + Width)/2. When tumors size reached ~500 mm^3, mice were randomly divided into different treatment groups, including: (1) 10 mg/kg*2 Taxol® for lymphoma model, and 10 mg/kg*4 TaxolR for breast tumor model, respectively; TaxolR was i.v. injected every other day from day 0 for indicated times; (2) Intratumoral injection of 10 mg/kg, 20 mg/kg or 40 mg/kg hydrogel in 50 μL volume; (3) Intratumoral injection of PBS vehicle control. The day giving drugs was designated as day 0. Mice weight was monitored after receiving treatment and presented as relative weight (%). Xenogen IVIS Lumina II system was used to perform bioluminescent imaging on 4T1-luciferase tumor-bearing mice, which were anesthetized with 3% isoflurane. Each mice was received i.p. injection of 3 mg D-luciferin, firefly, potassium salt (Caliper Life Sciences), prior to imaging.

2.7. Statistical analysis

Tumor model data are represented as Mean ± SEM. Tumor growth curve was compared and analyzed using the two-way analysis of variance test (ANOVA), performed by GraphPad Prism 5.01 for Windows. $^*p < 0.05$, $^{**}p < 0.01$ and $^{***}p < 0.001$ were used throughout the article to show statistical significance.

3. Results and discussion

3.1. Molecular design and hydrogel formation

Our group has reported several molecular hydrogelators of taxol derivatives [21,22]. During the preparation of aqueous solutions of taxol derivatives, we occasionally found that taxol derivatives would undergo an ester bond hydrolysis process to release the original taxol molecule, thus leading to the formation of molecular hydrogels. This observation stimulated us to design Taxol-SA-GSSG (**1** in Scheme 1) as the precursor of molecular gelator (taxol). We designed compound **1** because of the following reasons: 1) succinic acid (SA) and oxidized glutathione (GSSG) could be used *in vivo*, 2) GSSG was very hydrophilic and could enhance the solubility of compound **1** and 3) GSSG was commercial available, making the synthesis of compound **1** easy and straightforward.

After the preparation of compound 1 in high yield (overall yield = 80% in two steps), we tested its gelation ability upon keeping a phosphate buffer saline (PBS, pH 7.4) solution containing 2.0 wt% of compound 1 at room temperature (22–25 °C) or 37 °C (Fig. 1A). We observed the formation of hydrogels after about 6 h both at room temperature and 37 °C (Fig. 1B). The LC-MS results clearly indicated that about 57%, 90% and 95.4% of the ester bond between taxol and SA was self-hydrolyzed at gelling points, after 4 days and after 7 days, respectively. The speed of hydrolysis of ester bond was highly dependent on the pH value of solutions—faster at higher pH values and vice versa. And the pH value of solutions could not be higher than 8.0, otherwise, the ester bonds on taxol would also be hydrolyzed. The hydrogel was stable for more than six months at room temperature or at 4 °C in a refrigerator. And we did not observe any hydrolysis of ester bonds on taxol at room temperature for three months in hydrogels in PBS buffer solutions (pH = 7.4). The concentration range of 1 to gel PBS buffer solutions via hydrolysis process was 0.5–15.0 wt% (lower than 0.5 wt% led to clear solutions after one week and the maximum solubility of 1 was about 15 wt% in the PBS buffer solution). What we needed to point out was that taxol hydrogels could only form by the hydrolysis process but not other methods such as heating-cooling process and assistance with organic solvents. These observations clear indicated that taxol could form hydrogels via the hydrolysis process and

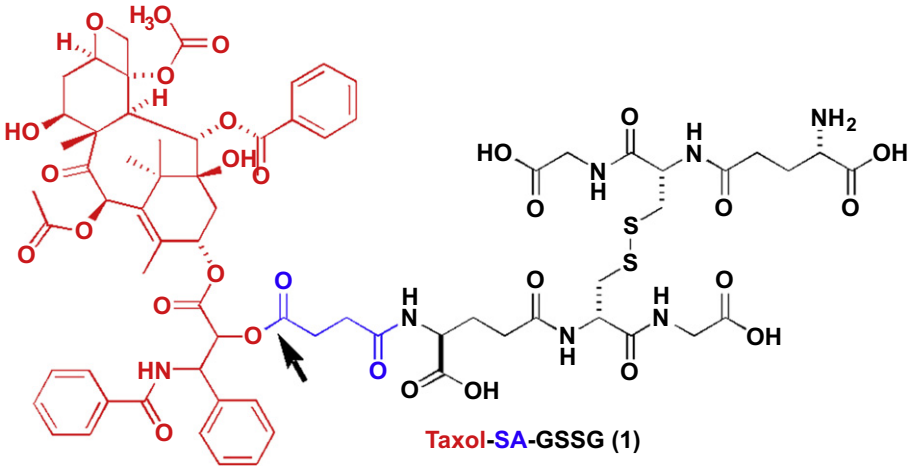

Scheme 1. Chemical structure of precursor of molecular hydrogelator (Taxol-SA-GSSG (**1**), red part: Taxol, blue part: succinic acid (SA) and black part: oxidized glutathione (GSSG)), compound **1** will undergo ester bond hydrolysis (indicated by the arrow) to release Taxol and lead to hydrogelations. (For interpretation of the references to colour in this figure legend, the reader is referred to the web version of this article.)

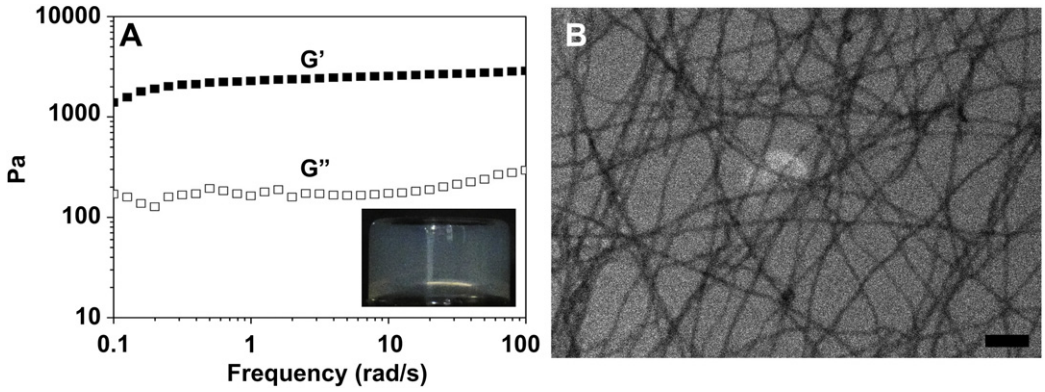

Fig. 1. A) Dynamic frequency sweep at the strain of 0.2% and at 37 °C (insert: an optical image) and B) a TEM image of a Taxol gel from a PBS solution containing 2.0 wt% of **1** (the scale bar in B represented 200 nm).

concentration of taxol in resulting gels could be managed in a wide range.

3.2. Rheometry

We then characterized the mechanical property of the hydrogels by a rheometer and tested whether gels were injectable or not. As shown in Fig. 1A, after the 24 h incubation of a PBS solution containing 2 wt% of **1** in the rheometer, a dynamic frequency sweep was performed at the strain of 0.2% and at 37 °C. The result showed that G′ value of the gel was about 2,200 Pa and one magnitude bigger than G″ value of the gel (200 Pa), indicating the formation of a true gel (Fig. 1A (insert)). The gels could be drawn into a syringe and then injected into a small vial from the syringe. And we could observe re-formation of a gel after 5 min (Figure S-3). These observations indicated that hydrogels of taxol formed by the hydrolysis process were injectable and could be administrated via injection to subcutaneous or i.t. spaces of animals.

3.3. Nanofibre morphology

The transmission electron microscopy (TEM) image provided useful information on morphology of self-assembled structures in the gel. As shown in Fig. 1B, we observed uniform nanofibers with width of about 25 nm and length of several microns. These nanofibers entangled with each to form three dimensional networks to support the hydrogel formation.

3.4. In vitro release profile

We studied the *in vitro* releasing profile of taxol from gels at physiological temperature condition (37 °C). A 0.25 mL of PBS buffer solution was added on top of 0.25 mL of gels formed from PBS solutions containing different concentrations of **1** (original concentration of **1** = 1.0, 1.5 and 2.0 wt%). The upper solutions were totally taken out at desired time points for measurement of accumulating release amount of taxol from gels and a fresh PBS buffer solution (0.25 mL) was then added. As shown in Fig. 1, three gels with different concentrations of taxol exhibited similar release profiles—they released taxol at a rate of about 1.4 μg per hour in the first 8 h and then at a relative lower rate of about 0.75 μg per hour in the following 16 h. We only observed taxol itself got released from gels formed after 4 days at 37 °C.

3.5. Minimum fatal dosage

We then evaluated the *in vivo* toxicity and anti-tumor efficacy of our hydrogels compared to clinically used i.v. injection of Taxol®. The minimum fatal dose was firstly studied for Taxol® and our hydrogels. As shown in Table S-1, i.v. injections of Taxol® at a single dose of more than 20 mg/kg caused serious toxicity to mice and it took more than 24 h for mice to re-gain normal activity (movement). An i.v. injection of Taxol® at a single dose of 40 mg/kg was fatal to mice, indicating that the fatal dose of clinical used Taxol® injection was between 20 and 40 mg/kg. Compared to Taxol® our hydrogels administrated to subcutaneous spaces of mice showed very low toxicity to mice at dosages of lower than 80 mg/kg of taxol, which was demonstrated by the normal body weight gain of mice in Figure S-6. Though a single subcutaneous administration of hydrogel at a dosage of 150 mg/kg would cause body weight loss in the first several days (Fig. 2), the fatal dosage of our hydrogels was higher than 300 mg/kg, which was at least 7.5 times higher than that of Taxol®. What we needed to point out was that subcutaneous injections of our gels at dosages higher than 40 mg/kg would lead to formation of wounds in the skin of mice after about 4–7 days

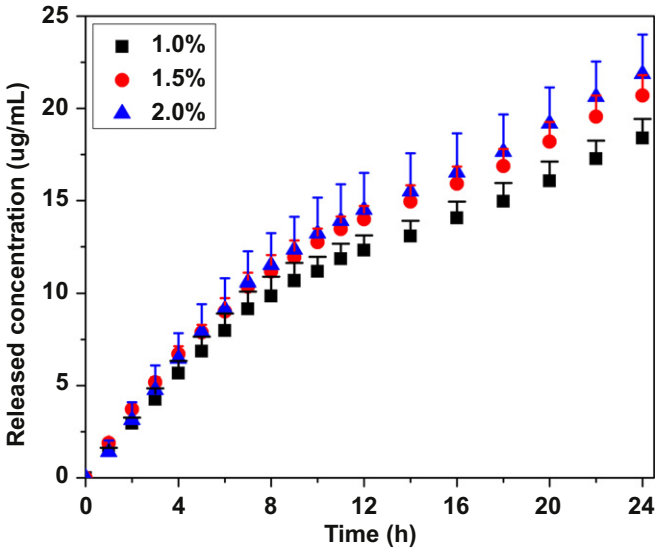

Fig. 2. Accumulative release profile of Taxol from different gels formed from solutions containing different concentrations of **1**, in 100 mM PBS buffers (pH = 7.4, n = 3, SD).

(Figure S-5) due to the unselected toxicity of taxol to all kinds of cells. This observation suggested that we could only apply our hydrogels in i.t. space at high dosages but not the subcutaneous space because wound infections would cause serious problems for patients in bad health conditions. In order to administrate our hydrogels in subcutaneous spaces of mice, the dosage should be lower than 20 mg/kg.

3.6. Anti-tumor efficacy

We then evaluated the *in vivo* anti-tumor efficacy of our hydrogels in two mice tumor models (EL-4 lymphoma tumors in subcutaneous spaces of right flank of mice and 4T1-luciferase breast tumors in mammary fat pad of female mice). When the volume of breast tumors reached about 435 mm^3, we injected different dosages (10, 20 and 40 mg/kg of taxol) of our hydrogels into tumors in the same volume (50 μL) by variation of the concentration of taxol in gels. As shown in Fig. 4A, our hydrogels could efficiently hinder tumors growth in a dose dependent way in the first 6 days and delayed the tumor growth in the following 6 days. The final volume of tumors was about 432% ($^{**}p = 0.0053$), 332% ($^{**}p = 0.0019$) and 273% ($^{***}p = 0.0008$) bigger than the original volume of tumors (435 mm3). However, the final relative tumor volumes were 610% (ns $p > 0.05$) and 865% in groups administrated with 40 mg/kg of Taxol® (i.v. Injection at a dosage of 10 mg/kg every other day) and i.t. injection of a PBS solution (50 μL) as control, respectively. These observations clearly indicated that our hydrogels of taxol could efficiently hinder the growth of breast tumors. Though the anti-tumor efficacy of our hydrogels to lymphoma tumors was not as high as that to breast tumors, our hydrogels could also hinder the growth of lymphoma tumors more efficiently than Taxol® injection at the same dosage (Fig. 4B).

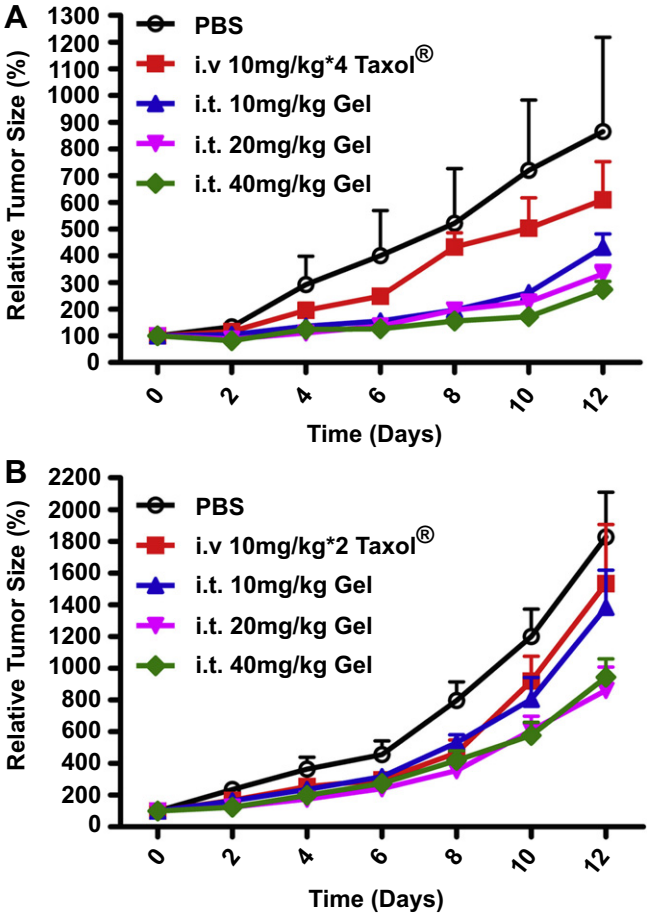

Fig. 4. A) Gels inhibit xenografted mouse breast tumor (4T1-luciferase) growth *in vivo* (gels were administrated into i.t. spaces after tumor sizes reaching 435 mm^3, $n = 6$) and B) gels inhibits xenografted mouse lymphoma (EL-4) growth *in vivo* (gels were administrated into i.t. spaces after tumor sizes reaching 524 mm^3, $n = 6$).

3.7. Metastasis inhibition

We also demonstrated that our hydrogels administrated directly into tumors could prevent metastasis of breast cancers. The breast cancer cell lines were stably transfected with a plasmid expressing luciferase. Therefore, the *in vivo* localization of cancer cells could be imaged via injection of a solution of luciferase substrate (D-luciferin). As shown in Fig. 5, Bright metastasis foci were observed in groups administrated with a PBS buffer solution (Fig. 5A and Figure S-9) or Taxol® intravenously injection at a dosage of 40 mg/kg (Fig. 3B) at day 12 after drugs treatment. Compared to the control groups, we did not observe obvious metastasis foci in mice administrated with gels at three different dosages (10, 20 and 40 mg/kg in Fig. 5C, 5D and 5E, respectively). The black spots within tumors (Fig. 5C–E and Figure S-9) also indicated that cancer cells in the inner part of tumors had been killed by high concentration of

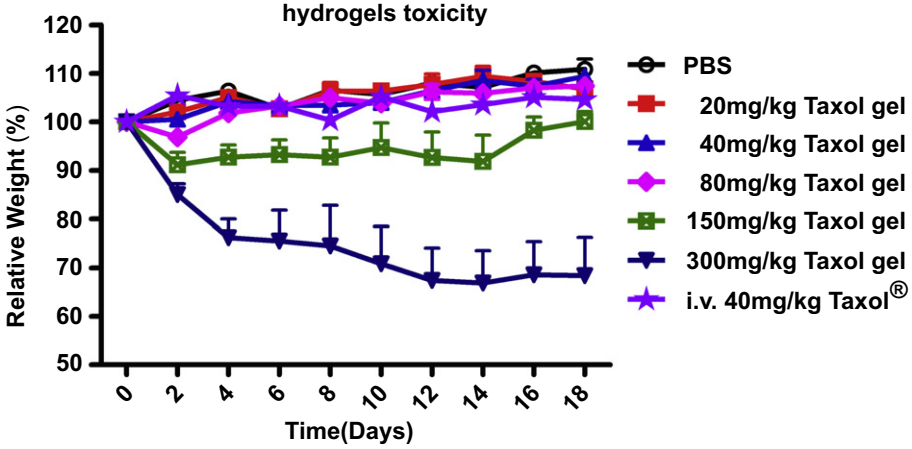

Fig. 3. In vivo toxicity performance of our hydrogels at different dosages compared with Taxol® ($n = 4$).

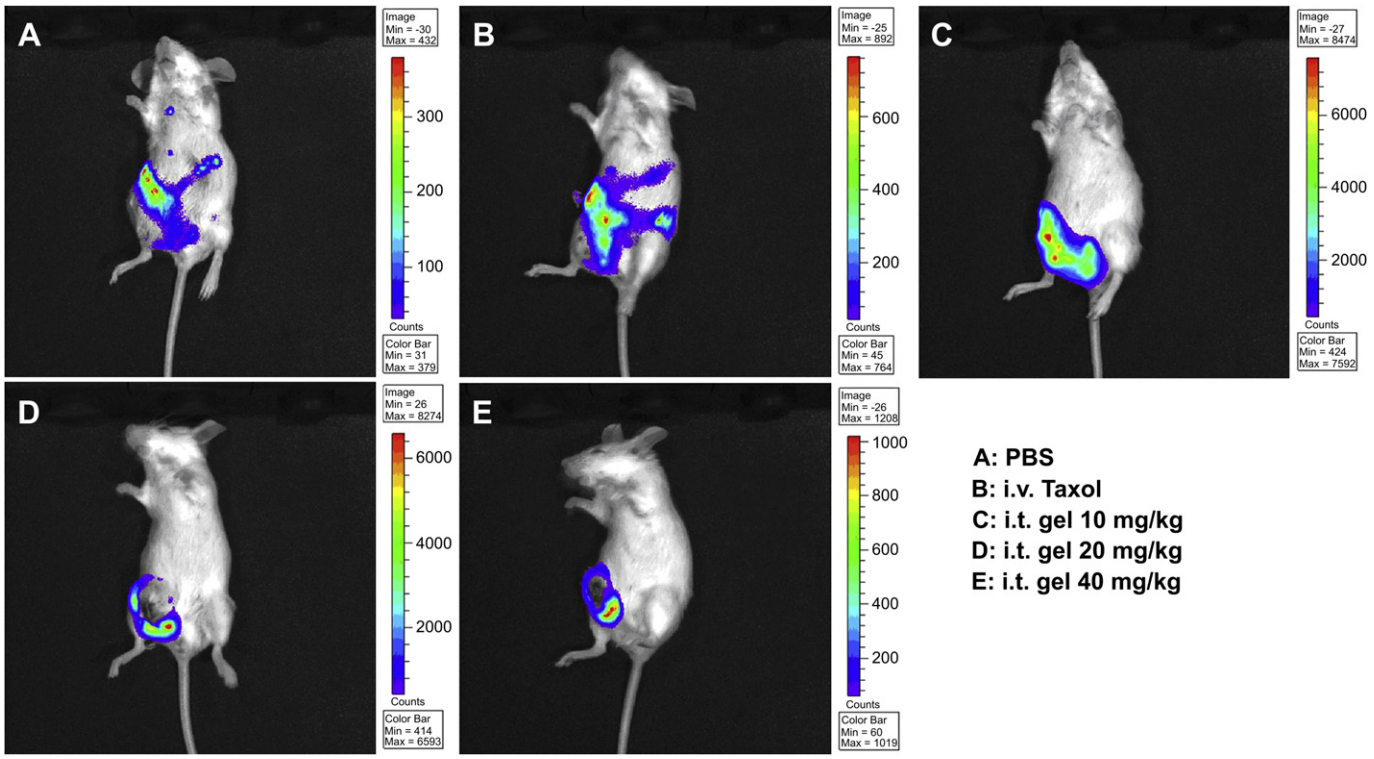

Fig. 5. Bioluminescent imaging on 4T1-luciferase tumor-bearing mice 12 days after given indicated treatment. Tumor cells are displayed with a red blue color bar, red color indicating the highest biolusminescence intensity. (For interpretation of the references to colour in this figure legend, the reader is referred to the web version of this article.)

taxol. The different size of light spots in five groups of mice in Fig. 5 correlated well with the results of tumor volumes obtained in Fig. 4A.

3.8. Body weight change of mice and plasma concentration of taxol

During the experiments to determine anti-tumor efficacy of our hydrogels against different tumors, we also monitored the body weight of the mice. We did not observe obviously body losses in groups of mice administrated with our hydrogels (Figure S-7 and S-8), compared to the control group of mice without any treatments, which was consistent with the results in Fig. 3 that mice administrated with our hydrogels at dosages lower than 80 mg/kg would have normal body weight gains. The high biocompatibility of our hydrogels at high dosages was due to the way of local delivery, thus leading to the low concentration of taxol in the circulation system of mice (blood)—the concentration of taxol in blood was 400–100 ng/mL in the first 3 days and dropped down below the minimum therapeutic effective level (43 ng/ml) at day 5 (Figure S-6) for mice administrated with different dosages of our hydrogels (10, 20 and 40 mg/kg). The low concentration of taxol in blood suggested that local administration of our hydrogels might reduce side effects to normal tissues.

4. Conclusion

In summary, we have developed a molecular hydrogel mainly composed of taxol itself, which could be administrated into solid tumors to hinder their growths and prevent their metastasis. The low blood concentration of taxol and high anti-cancer efficacy of our hydrogels suggested the great potential of the gels for chemotherapy. Our hydrogel of taxol was only a new administration form of the clinically used Taxol® injection, which suggested its big possibility for the practical application. Though we only reported the results about molecular hydrogels formed through the hydrolysis of compound **1** with a hydrophilic part of GSSG, other hydrophilic molecules such as PEG could also be used for the construction of precursor of taxol, which would push forward in a further step the practical application of our taxol hydrogel. We are currently actively investigating the possibility of our taxol hydrogel for practical application.

Acknowledgment

This work is supported by NSFC (30890143) ands Key Program for International S&T Cooperation Projects of China (2010DFB34000) to Yin group and NSFC (31070856) and Tianjin MSTC (11JCZDJC17200) to Yang group.

Appendix. Supplementary material

Supplementary material associated with this article can be found, in the online version, at doi:10.1016/j.biomaterials.2012.04.047.

References

[1] Marupudi NI, Han JE, Li KW, Renard VM, Tyler BM, Brem H. Paclitaxel: a review of adverse toxicities and novel delivery strategies. Expert Opin Drug Saf 2007;6(5):609–21.
[2] Shen YQ, Jin EL, Zhang B, Murphy CJ, Sui MH, Zhao J, et al. Prodrugs forming high drug loading multifunctional nanocapsules for intracellular cancer drug delivery. J Am Chem Soc 2010;132(12):4259–65.
[3] Greenwald RB, Choe YH, McGuire J, Conover CD. Effective drug delivery by PEGylated drug conjugates. Adv Drug Deliver Rev 2003;55(2):217–50.
[4] Safavy A, Georg GI, Vander Velde D, Raisch KP, Safavy K, Carpenter M, et al. Site-specifically traced drug release and biodistribution of a paclitaxel-antibody conjugate toward improvement of the linker structure. Bioconjug Chem 2004;15(6):1264–74.

[5] Kukowska-Latallo JF, Candido KA, Cao ZY, Nigavekar SS, Majoros IJ, Thomas TP, et al. Nanoparticle targeting of anticancer drug improves therapeutic response in animal model of human epithelial cancer. Cancer Res 2005;65(12):5317–24 (in English).
[6] Thierry B, Kujawa P, Tkaczyk C, Winnik FM, Bilodeau L, Tabrizian M. Delivery platform for hydrophobic drugs: prodrug approach combined with self-assembled multilayers. J Am Chem Soc 2005;127(6):1626–7.
[7] Nie SF, Hsiao WLW, Pan WS, Yang ZJ. Thermoreversible pluronic (R) F127-based hydrogel containing liposomes for the controlled delivery of paclitaxel: in vitro drug release, cell cytotoxicity, and uptake studies. Inter J Nanomed 2011;6:151–66.
[8] Yu X, Pishko MV. Release of paclitaxel from pH sensitive and biodegradable dextran based hydrogels. Soft Matter 2011;7(19):8898–904.
[9] Ma N, Xu HP, An LP, Li J, Sun ZW, Zhang X. Radiation-Sensitive Diselenide block co-polymer Micellar Aggregates: toward the combination of radiotherapy and chemotherapy. Langmuir 2011;27(10):5874–8.
[10] Bellomo EG, Wyrsta MD, Pakstis L, Pochan DJ, Deming TJ. Stimuli-responsive polypeptide vesicles by conformation-specific assembly. Nat Mater 2004;3(4):244–8.
[11] Cheng WL, Park NY, Walter MT, Hartman MR, Luo D. Nanopatterning self-assembled nanoparticle superlattices by moulding microdroplets. Nat Nanotech 2008;3(11):682–90.
[12] Liu LH, Xu KJ, Wang HY, Tan PKJ, Fan WM, Venkatraman SS, et al. Self-assembled cationic peptide nanoparticles as an efficient antimicrobial agent. Nat Nanotech 2009;4(7):457–63.
[13] Du JZ, Du XJ, Mao CQ, Wang J. Tailor-made dual pH-sensitive polymer-doxorubicin nanoparticles for efficient anticancer drug delivery. J Am Chem Soc 2011;133(44):17560–3.
[14] Huang CC, Huang W, Yeh CS. Shell-by-shell synthesis of multi-shelled mesoporous silica nanospheres for optical imaging and drug delivery. Biomaterials 2011;32(2):556–64.
[15] Nicolaou KC, Guy RK, Pitsinos EN, Wrasidlo W. A water-soluble prodrug of taxol with self-assembling properties. Angew Chem Int Ed 1994;33(15–16):1583–7.
[16] Soukasene S, Toft DJ, Moyer TJ, Lu HM, Lee HK, Standley SM, et al. Antitumor activity of peptide amphiphile nanofiber-encapsulated camptothecin. ACS Nano 2011;5(11):9113–21.
[17] Altunbas A, Lee SJ, Rajasekaran SA, Schneider JP, Pochan DJ. Encapsulation of curcumin in self-assembling peptide hydrogels as injectable drug delivery vehicles. Biomaterials 2011;32(25):5906–14.
[18] Vemula PK, Cruikshank GA, Karp JM, John G. Self-assembled prodrugs: an enzymatically triggered drug-delivery platform. Biomaterials 2009;30(3):383–93.
[19] Vemula PK, Li J, John G. Enzyme catalysis: Tool to make and break amygdalin hydrogelators from renewable resources: a delivery model for hydrophobic drugs. J Am Chem Soc 2006;128(27):8932–8.
[20] Gao Y, Kuang Y, Guo ZF, Guo ZH, Krauss IJ, Xu B. Enzyme-instructed molecular self-assembly confers nanofibers and a supramolecular hydrogel of taxol derivative. J Am Chem Soc 2009;131(38):13576–7.
[21] Wang HM, Yang CH, Wang L, Kong DL, Zhang YJ, Yang ZM. Self-assembled nanospheres as a novel delivery system for taxol: a molecular hydrogel with nanosphere morphology. Chem Commun 2011;47(15):4439–41.
[22] Mao LN, Wang HM, Tan M, Ou LL, Kong DL, Yang ZM. Conjugation of two complementary anti-cancer drugs confers molecular hydrogels as a co-delivery system. Chem Commun 2012;48:395–7.
[23] Maji SK, Schubert D, Rivier C, Lee S, Rivier JE, Riek R. Amyloid as a depot for the formulation of long-acting drugs. PLoS Biol 2008;6:240–52.
[24] Valery C, Paternostre M, Robert B, Gulik-Krzywicki T, Narayanan T, Dedieu JC, et al. Biomimetic organization: Octapeptide self-assembly into nanotubes of viral capsid-like dimension. Proc Natl Acad Sci USA 2003;100(18):10258–62.